HHS Public Access

Author manuscript

Wiley Interdiscip Rev Syst Biol Med. Author manuscript; available in PMC 2017 May 01.

Published in final edited form as:

Wiley Interdiscip Rev Syst Biol Med. 2016 May ; 8(3): 211–226. doi:10.1002/wsbm.1330.

Mathematical Modeling of Cardiac Growth and Remodeling

L.C. Lee[a], **G.S. Kassab**[b], and **J.M. Guccione**[c]

[a]Department of Mechanical Engineering, Michigan State University, East Lansing, MI, U.S.A.

[b]California Medical Innovations Institute, San Diego, CA, U.S.A.

[c]Department of Surgery, University of California at San Francisco, San Francisco, CA, U.S.A.

Abstract

This review provides an overview of the current state of mathematical models of cardiac growth and remodeling (G&R). We concisely describe the experimental observations associated with cardiac G&R and discuss existing mathematical models that describe this process. To facilitate the discussion, we have organized the G&R models in terms of (1) the physical focus (biochemical vs. mechanical) and (2) the process that they describe (myocyte hypertrophy vs. extracellular matrix remodeling). The review concludes with a discussion of some possible directions that can advance the existing state of cardiac G&R mathematical modeling.

Keywords

Cardiac growth and remodeling; mathematical modeling; hypertrophy; fibrosis; extracellular remodeling

1. Introduction

The heart is a highly complex living structure consisting of a collection of cells (e.g., myocytes, myofibroblasts, endothelial cells, vascular smooth muscle cells) and extracellular constituents (e.g., collagen fibers and proteoglycans). The primary function of the heart is to cyclically contract in order to generate a pressure gradient to perfuse all body organs including itself. To do so, however, the myocardium must operate as a system where all the individual constituent (or sub-system) operations are tightly orchestrated.

In response to neurohormonal, chemical and mechanical cues, the myocardium can undergo long term adaptive or maladaptive processes that are commonly referred to as “growth and remodeling” (G&R). Growth and remodeling can be a manifestation of many sub-processes that occur at a smaller scale, including cellular hypertrophy, apoptosis, proliferation, and extracellular matrix remodeling[1]. Collectively, these sub-processes lead to geometrical and functional changes of the heart, which can have significant clinical implications.

Myocardial G&R is widely considered to be an important determinant of the clinical course of heart failure[2]. As heart failure progresses, the heart size increases and its function deteriorates. Indeed, multiple studies have shown that an increase in heart size is associated

with an adverse prognosis in many heart diseases[3,4]. By the same logic, a reversal of pathological G&R features in the form of a reduction in the heart size is widely considered to be a favorable response to treatments. This process, often referred to as reverse remodeling, and has been observed in numerous treatments that include prolonged support by left ventricular assist device[5,6], bio-injection therapies[7,8] and cardiac resynchronization therapy[9,10].

Despite their clinical importance, our current understanding of the myocardial G&R mechanisms remain rudimentary. For example, the type of mechanical signals that myocytes sense (whether is it stress or strain[11] or strain energy) and the way they respond to these signals (how their geometry and function changes) have not been fully elucidated[12–14]. A clear understanding of the various mechanisms of myocardial G&R and how they interact with one another may provide key insights for developing effective heart failure therapies. Given the complexity of the multitude of G&R pathways and their interactions, mathematical modeling has emerged as a powerful tool to make the problem more tractable. This is especially effective when mathematical models are coupled together with experiments in an iterative fashion to generate and test new hypotheses of G&R.

Here, our goal is to provide an overview of the state of the art in mathematical models of myocardial G&R. We briefly characterize myocardial G&R and then review existing mathematical models. We have categorized the models according to their focus on G&R pathways (biochemical vs. mechanical) and processes (cellular hypertrophy vs. remodeling of the extracellular matrix (ECM)). Finally, we call attention to how these mathematical models can be advanced so that G&R can be understood at a system-level.

2. Myocardial Growth and Remodeling

Myocardial G&R can be broadly defined as changes in the heart geometry and function that occur over a period of time that is significantly longer than a heartbeat. The nature of G&R can be pathological (e.g., in heart diseases) or physiological (e.g., during growth and development, exercise, pregnancy, ageing, etc.). In some cases, the G&R response can be quite similar under both circumstances. For instance, cellular hypertrophy in response to pressure overloading occurs in both hypertensive heart disease and during postnatal heart development. Under pathophysiological conditions, G&R may initially behave as a compensatory mechanism to normalize function in response to pathological stimuli. This is widely believed to be the case when left ventricular (LV) wall thickness increases during pressure overloading, which normalizes the wall stress[15]. Over time, however, the (usually asymptomatic) compensatory state gives way to a decompensated state that progresses to heart failure. The exact mechanisms responsible for the transition from compensated to decompensated G&R are not fully understood and are under intense investigation[16].

Classically, G&R in the myocardium is categorized into two types based on the LV geometry: concentric and eccentric hypertrophy. During concentric hypertrophy, the LV wall thickens and there is little change in the chamber volume whereas during eccentric hypertrophy, the LV wall thins and the chamber volume increases significantly[17]. The LV also becomes more spherical in the latter. The ultrastructural basis that gives rise to these

two types of geometrical features has been associated with the way sarcomeres are added in myocytes. Specifically, thickening of the LV wall and dilation of the LV chamber are due to the parallel and serial addition of sarcomeres in the myocytes, respectively. The fact that the resultant ventricular shape is largely determined by changes in myocyte shape is not surprising for three reasons. First, myocytes account for the bulk (75%) of the myocardial mass[18]. Second, myocytes are highly organized with their long axis mostly orthogonal to the myocardial transmural direction. Last, myocytes in the adult human heart regenerate at an extremely slow rate in which only about 50% are exchanged during the normal life span[19].

In addition to geometrical changes, G&R can also induce functional changes that affect myocardial contraction. These changes can occur in the cardiac tissue's bulk mechanical and electrical properties, such as contractility, passive stiffness and electrical conduction velocity. During G&R, the myocyte contractile function, which modulates the heart systolic function, may be altered. Myocyte hypertrophy has been associated with both an increase and a decrease in contractile function. This disparity in functional changes during hypertrophy has been attributed to the different phases of G&R; namely, the compensated and the decompensated phases[20]. In addition to the contractile function, G&R can also perturb the tissue's passive stiffness. Myocardial stiffness plays a central role in the heart's diastolic function, whereby an excessive increase in stiffness can impair diastolic filling, a hallmark of diastolic heart failure with preserved ejection fraction. Such an increase in myocardial tissue stiffness has been attributed to a delayed relaxation of the myocyte's contraction as well as an increase in the intrinsic myocardial stiffness[21]. The latter may be associated with an alteration of the myocardial collagen fiber network in the ECM[21,22].

The highly complex fibrillar collagen network in the myocardial ECM provides structural integrity to the adjoining myocytes. In addition to a network of collagen fiber, the ECM also contains other matrix proteins such as proteoglycans, glycosaminoglycan, and other signaling molecules such as angiotensin II[22]. Scanning electron microscopy has revealed extensive collagen fibrillar weaves that surround and support individual myocytes[23,24]. Due to the tight connections between myocytes and the collagen network, the ECM likely serves as a conduit for mechanical (stresses and strains) signal transmission to the cells, in addition to providing structural support for the myocardium. Therefore, any changes in the structure and composition of the ECM would not only contribute to the overall myocardial G&R process (e.g., stiffening of the tissue), but it would also have an impact on the cellular remodeling response. In addition, excessive extracellular collagen fiber accumulation also leads to a decrease in myocardial conduction velocity[25], and an increase in arrhythmia[26].

The majority of changes during myocardial G&R can be traced to the geometrical and functional changes in the myocytes, as well as changes in the myocardial collagen fiber network. For this reason, mathematical models of myocardial G&R are mainly constructed to describe these events.

3. Biochemical Models of Growth and Remodeling

3.1 Hypertrophy

A variety of hypertrophic stimuli such as mechanical cues (e.g., stresses and strains) and chemical agents (e.g., cytokines, growth factors, catecholamines, vasoactive peptides, hormones and many others) have been identified in myocytes[27]. Mathematical models have been constructed to describe and elucidate the signaling pathways associated with these hypertrophic stimuli[13,28,29]. For mechanotransduction pathways, Novak et al.[30] proposed a model based on reaction kinetics that predicts the focal adhesion distribution in a cell in response to a force field. In a subsequent work, Grosberg et al.[31] extended that model to include the fiber-length force dependency to describe the kinetics of myofibrillogenesis. Other approaches to describe the focal adhesions kinetics include a thermodynamically consistent model proposed by Deshpande et al.[32]. A number of models have also been constructed to describe the signaling pathways of non-mechanical hypertrophic stimuli. For example, Shin et al.[29] constructed a mathematical model to describe the signaling pathway between calcineurin and the nuclear factor of activated T-cells, whereas Cooling et al.[28] constructed a model to describe the IP3 signal production by extracellular agonists endothelin-1 and angiotensin-II.

To assimilate the various pathways and stimuli of myocyte hypertrophy, Ryall et al.[33] described a computational model of the hypertrophic signaling network that integrates many of the established pathways. This extensive network (consisting of 193 reactions and 106 species) was described using logic-based differential equations that represent activation and inhibition of reactions with normalized Hill functions. A sensitivity analysis was performed on the model, which identified species with the greatest effects on myocyte hypertrophy and revealed 12 major functional signaling modules. The model identified Ras as a primary network hub that has the greatest influence on hypertrophy, suggesting that the inhibition of cardiomyocyte hypertrophy could be better achieved by blocking Ras. This finding was validated experimentally in the same study. Contrary to experimental studies focusing on specific isolated hypertrophic signaling pathways[34,35], this model demonstrates the ability of mathematical modeling as a tool to analyze a complex system that would otherwise be nearly impossible with experiments that focus on specific hypertrophic signaling pathways. The model could, in principle, also be used to identify drug targets for hypertrophy[36]. To do so, however, future studies are needed to measure the parameters (which were prescribed with default values for all the reactions in the network) to avoid ad hoc assumptions.

3.2 Extracellular remodeling

Mathematical models describing the remodeling process in the ECM are scarce. Although some models have been constructed to investigate a specific pathway of ECM remodeling (e.g., degradation of collagen fibers by MMPs[37,38]), system-level mathematical models that take into account the multiple signaling pathways during ECM remodeling are lacking. Given that this process is most prominent during the development of myocardial infarction, it is not surprising that existing models are mostly developed under this pathological setting. Based on mice with coronary artery ligation, Jin et al.[39] developed a mathematical model to describe the post-MI scar formation process. In their ECM model, the time course of key

chemical factors post-MI (i.e., macrophage cell density, fibroblast cell density, collagen concentration, TGF-β and activated MMP-9 concentration) were described using a set of coupled ordinary differential equations (ODEs) (Figure 1). The model predictions of macrophage, MMP9 and fibroblast expressions are in good agreement with other published experiments[40–42]. Using the validated parameter values, the model predicted that an early intervention of elevating the MMP-9 level immediately after myocardial infarction will significantly decrease the resultant collagen density when compared to a later intervention. With further development, the mathematical model may be useful in elucidating the quantitative effects of MMP inhibitors that are currently investigated as a therapy to prevent post-MI LV remodeling[43].

4. Mechanical models of G&R

The models discussed thus far focus primarily on the local cellular-scale biochemical reactions that occur during G&R. These reactions were mostly described using coupled ODEs of first-order reaction kinetics. As such, there is no length scale in the equations for describing the spatial variation of quantities such as the concentration of collagen fibers and size of myocytes. These models also do not directly predict changes in the geometry, structure and mechanical properties of the myocardium during G&R. The geometric, structural and material changes are important as they have direct implications on the cardiac function. Mathematical models of myocardial G&R that can account for these changes are typically constructed at the tissue- and organ-level using the principles of continuum mechanics. These models can be broadly classified based on their origins into: (1) structural adaption theory, (2) volumetric growth theory and (3) constrained mixture theory.

4.1 Structural adaption theory

One of the first cardiac G&R model that considers the (structural) remodeling of myofiber orientation, in addition to geometrical remodeling, was described by Arts et al.[44]. Using a heart model consisting of adjoining cylindrical shells, the myofiber orientation (in addition to the wall thickness) was adapted in each shell to optimize the local deviation of (1) the fiber shortening during systole and (2) the sarcomere length at the beginning of ejection from their corresponding prescribed set points. Their model yielded a transmural variation of myofiber orientation that is consistent with those found experimentally. A subsequent study by Kroon et al.[45] using a finite element model of a truncated ellipsoid also produced the same result, though with a different remodeling law in which the myofibers adapt their direction to minimize the fiber-cross fiber shear strain. We refer readers to the review by Bovendeerd[46] for a discussion of this class of models that describe the remodeling of myofiber orientation.

4.2 Volumetric growth theory

First proposed by Rodriguez et al.[47], the volumetric growth theory is the most prevalent framework for modeling G&R in myocardial tissue. This theory draws from the concept of decomposing the deformation gradient tensor multiplicatively into an elastic component and a plastic component in finite strain plasticity[48]. Analogous to this, the deformation gradient

tensor **F** is split into an elastic deformation gradient tensor $\mathbf{F}^{e}$ and a growth deformation gradient tensor $\mathbf{F}^{g}$ in the volumetric growth theory as:

$$\mathbf{F}=\mathbf{F}^{e}\cdot\mathbf{F}^{g}. \quad (1)$$

The growth deformation gradient tensor $\mathbf{F}^{g}$ is in general, “incompatible", which means that it is impossible to derive a unique displacement field from the tensor $\mathbf{F}^{g}$ itself. The compatibility condition as required by the deformation gradient tensor **F** is restored by the elastic component of the deformation gradient tensor $\mathbf{F}^{e}$. In this theory, the direct consequence of the incompatibility of $\mathbf{F}^{g}$ is that non-homogeneous growth in a body may generate residual stresses and strains[a]; i.e., stresses and strains that exist in the body without any external load[49]. This prediction is consistent with the fact that a residual stress/strain field is always present in the intact ventricular walls[49,50]. However, the existence of residual stress/strain may not only be due to G&R, as this feature can also be induced by other competing mechanisms[51] such as tissue swelling[52].

The growth deformation gradient tensor $\mathbf{F}^{g}$ can be interpreted as a change in the tissue stress-free configuration. The geometric changes associated with G&R during cellular hypertrophy and atrophy are most naturally described by this configurational change in which the elastic strains (i.e., strains that generate stresses) are taken with respect to this new configuration. Specifically, the tensorial form of $\mathbf{F}^{g}$ reflects changes in cell geometry due to the parallel and/or serial addition of sarcomeres as they undergo hypertrophy or atrophy (Figure 2). A constitutive relationship is required for the growth deformation gradient tensor $\mathbf{F}^{g}$ to link the geometrical changes (effects) to the stimulus (cause).

In recent years, a number of constitutive models have been developed under the volumetric growth framework to simulate myocardial G&R under various physiological and pathological conditions. Taber and colleagues have constructed growth constitutive models to describe G&R in the developing heart[53,54]. In their models, growth was described by an ODE equation that can be generalized as $\dot{\mathbf{F}}^{g}=\mathbf{A}:(\mathbf{S}-\mathbf{S_0})$[55], where the rate of change of the growth deformation gradient tensor $\dot{\mathbf{F}}^{g}$ is driven by a deviation of the growth stimulus **S** from its homeostatic or target value $\mathbf{S_0}$. The growth stimulus was prescribed to be the stress tensor in their model and the fourth-order tensor **A** contains coefficients that control the growth-rate. This particular form has also been used by Kerckhoffs[56] and Kroon et al.[57] to simulate cardiac growth in the LV, but with myofiber and cross-myofiber normal strains as the growth stimuli. The unloaded configuration (which typically does not exist *in vivo*) was used as a reference state for the calculation of the strains as an input in most strain-driven growth constitutive models. This reference state is likely to change during G&R. As discussed by Rodriguez et al.[47] and Taber[58], however, the issue of which reference state to use would not arise if Cauchy stress, which does not depends on the choice of a reference configuration, is used as a growth stimuli.

The form $\dot{\mathbf{F}}^{g}=\mathbf{A}:(\mathbf{S}-\mathbf{S_0})$ assumes that (1) the growth rate is a linear function of the stimulus and (2) the amount of growth is not constrained by any physiological limit; i.e.,

[a]There are special cases in which non-homogeneous growth does not generate residual stresses.

growth (or shrinkage) continues as long as $\mathbf{S} \neq \mathbf{S_0}$. Models not adhering to these assumptions have also been developed. Based on the conventional hypothesis that myocardial wall stress and strain are, respectively, the stimulus causing concentric and eccentric cardiac hypertrophy during pressure and volume overload, Goktepe et al.[59] described separate growth constitutive models to simulate these two conditions. In their model, growth in the myofiber and cross-fiber directions were driven by a deviation of the myofiber stretch and the Mandel stress from their corresponding homeostatic set point. A rate-limiting function was used to restrict growth to within prescribed physiological limits. Goktepe et al.[59] showed that key G&R features during pressure overload (wall thickening) and volume overload (chamber dilation) can be predicted using their models. This strain-driven growth model was further extended by Lee et al.[60] to simulate a reversal of G&R in response to a reduction in hemodynamic load that can be found, for example, after the implantation of left ventricular assist device. This model has also been integrated with cardiac electromechanics[61]. Contrary to the prevailing hypothesis that concentric and eccentric hypertrophy are caused separately by an elevated myocardial stress and strain, respectively, Kerckhoffs et al.[62] constructed a growth constitutive model in which the different components of myocardial strain tensors are used as growth stimuli. In their model, growth rates in the myofiber and cross myofiber directions were described by nonlinear sigmoidal functions of growth stimuli, which were the deviation of myofiber and cross myofiber strains from their corresponding homeostatic set points. In this model, growth was also restricted to lie within a prescribed physiological limit. Kerckhoffs et al.[62] showed that by using these quantities as growth stimuli, the model can reproduce key G&R features associated with both concentric and eccentric hypertrophy. The issue of myocardial stress or strain as a mechanical stimulant for G&R is still under debate[11], although a number of studies have leaned towards strain or stretch as the responsible mechanical stimulant for G&R[63,64]. In one of these studies, Holmes[14] found that features of the time-varying signals, which include strain-related LV cavity volume amplitude and its rate of change, were significantly altered during early volume overload in rats. Based on this findings, he concluded that these mechanical signals are candidates for G&R mechanical stimuli. The issue of the true mechanical stimulant for G&R is not easily resolvable. But with the development of more growth constitutive models, various hypothesis can be formulated and tested by corroboration with experiment data.

Although growth constitutive models constructed based on a volumetric growth framework can predict geometrical changes, they cannot directly account for changes in the tissue mechanical properties found in the heart during G&R. These changes can be associated with a change in the ratio of the tissue constituent (e.g., fibrosis[1,65]) or a change in the intrinsic material property of the constituent (e.g., a change in myocyte stiffness[66] and contractile function[67]). As described by Taber[58], existing tissue material constitutive models describing its stress-strain relationship need to be reformulated with an additional input from the growth tensor $\mathbf{F}^{\boldsymbol{g}}$ in order for volumetric G&R–based models to account for any change in the tissue mechanical properties during G&R. To date, none of the volumetric growth-based constitutive models have accounted for this change and this remains a laudable goal of future efforts.

4.3 Constrained mixture theory

Subsequent to the volumetric growth theory, a separate theoretical framework based on the constrained mixture theory was formulated by Humphrey and Rajagopal[68] to model G&R. This theoretical framework was built upon the hypothesis that each tissue constituent, such as muscle cell and collagen fiber, can turnover at different rates and possess different natural/stress-free configurations that evolve during G&R while being constrained to deform as a continuum within the mixture (henceforth the name "constrained mixture"). One of the key hypotheses in this theory is that the deposition of new constituents such as collagen fibers always occurs at the current configuration. Referring to Figure 3, a constituent of type k (e.g., collagen fibers) deposited at time τ with a homeostatic stretch $\mathbf{G}^k(\tau)$ will experience a deformation described by $\mathbf{F}_{\boldsymbol{n}(\tau)}(t) = \mathbf{F}(t)\mathbf{F}^{-1}(\tau)\mathbf{G}^k(\tau)$ at a later time t in the configuration $\boldsymbol{\kappa}(t)$. Thus, newly deposited constituents will experience a different stress/strain state than that experienced by previously deposited constituents, even if they are of the same type. By consolidating the effects of all the constituents produced up to the current configuration at time t, the partial stress associated with constituent type k is given as:

$$\boldsymbol{\sigma}^k(t) = 1/\det\,\mathbf{F}_{\boldsymbol{n}(\mathbf{0})}(t) \int_{-\infty}^{t} m(\tau) G(t-\tau) \mathbf{f}(\mathbf{F}_{\boldsymbol{n}(\tau)}(t))\,\det\,\mathbf{F}_{\boldsymbol{n}(\mathbf{0})}(\boldsymbol{\tau}) d\tau. \quad (2)$$

Here, $m(\tau)$ is the mass production rate, $G(t-\tau)$ is the prescribed "survival" function for the constituent produced at time τ and $\mathbf{f}(\cdot)$ is the stress response function. The "survival function" describes the constituent's degradation time-course starting from birth time at τ to current time t. A key feature of this model is that it allows the tissue mechanical property to change during G&R without the need to reformulate the existing material constitutive descriptor (stress-strain relationship) of the constituents.

Compared to the volumetric growth theory, the constrained mixture model is relatively more complex to work with, in part, because of the need to track the evolving natural configuration of the constituents during G&R. As such, the application of constrained mixture G&R framework has, so far, been mostly confined to modeling arterial G&R using simplified geometry; e.g., approximating the arterial wall as a thin-wall membrane[69–71]. Although this model has not been applied to the heart, the theoretical framework is highly relevant and should be adapted to model myocardial G&R. This is because collagen deposition and degradation, the major focus of this theory, is an important aspect of myocardial G&R that has been observed in many heart diseases. For a more general review of continuum mixture-based models, including those applied to other biological tissues, we refer the readers to the review by Ateshian and Humphrey[72].

5. System Growth and Remodeling

Although mathematical models of myocardial G&R have advanced over the years, much work is needed to refine, improve and integrate these models. The following is a discussion of directions that can be undertaken to advance mathematical models of myocardial G&R.

5.1 Model Testing, Calibration and Validation

Most myocardial G&R models are not calibrated using experimental studies specifically designed for such a purpose. Instead, model parameters are largely estimated using previous experimental studies typically designed for a different purpose. As such, the experiments may not fully explore the variable space that is necessary to calibrate and test the models. For example, ventricular pressure is typically not varied over a large range in chronic experiments beyond hypertensive and baseline levels. This limitation may pose a problem where the number of experimental data points is insufficient to calibrate and test the growth constitutive models, particularly, in models where G&R is stress-mediated.

The number of parameters in the G&R models discussed in this review is listed in Table 1. In general, these parameters can be categorized based on their association with biochemical reaction rates, growth/mass production rates and limits/threshold/homeostatic states associated with G&R. The chemical rates (unit: s^{-1}) can be discerned from the growth/mass production rates (unit: $days^{-1}$) in terms of their timescales. As shown in the Table, the number of parameters can range between 8 to more than 100 in these models. This large number of parameters can, in effect, render the whole process of model testing, calibration and validation a complex task.

Perhaps a way to manage the complexity of this process in some of these models is to reduce them to the simplest form while retaining their primary hypothesis. To illustrate this point, we consider the simplification of a volumetric growth-based stress-mediated G&R constitutive model[53,73]. The hypothesis in the model is that growth (in the form of a change in wall thickness) occurs for the purpose of normalizing ventricular wall stress. Using standard Laplace's law to calculate the wall stress, the time-rate of a change in the wall thickness $\Delta\bar{h}$ can be reduced to the following ODE:

$$\Delta\dot{\bar{h}} = KP_o\left(\frac{1+\bar{P}}{(\bar{h}+\Delta\bar{h})(2+\bar{h}+\Delta\bar{h})} - \frac{1}{\bar{h}(2+\bar{h})}\right), \quad (3)$$

where K is the growth rate constant, P_o is the pre-growth pressure, $\bar{h}$ is the pre-growth wall thickness and $\bar{P}$ is the change in pressure (see Appendix for details). Dimensions and pressure in the equation have been normalized to the internal LV chamber radius and P_o, respectively. The only model parameter in this model is the growth rate constant K.

5.1.1 Testing the Model Hypothesis—In the model, steady state $(\Delta\dot{\bar{h}} = 0)$ occurs when the wall stress is restored. Under this condition, we find that the change in wall thickness $\Delta\bar{h}$ is a function of the pressure change $\bar{P}$ and pre-growth wall thickness $\bar{h}$ by

$$\Delta\bar{h} = -1 - \bar{h} + \sqrt{1+2\bar{h}+2\bar{P}\bar{h}+\bar{h}^2+\bar{P}\bar{h}^2}. \quad (4)$$

To test whether the model hypothesis agrees with the general observations of G&R, we plot this non-dimensionalized functional relationship (for the experimental range of $0.2 \le \bar{h} \le 0.7$) with data points collected from different existing experimental and clinical studies of different species during LV pressure-overload (Figure 4a)[74–78]. These data are given in the

Appendix. As shown in the figure, the data gathered from experiments conducted on different species are, in general, compatible with this simplified model and fall within the range of the experimental values of $\bar{h}$. On the other hand, the disparity between the model prediction and experiment is greater in some cases if the comparison was made based on the specific normalized wall thickness $\bar{h}$ of each experiment. More data points are needed to ascertain this compatibility. In the plot, we have implicitly assumed that a steady state condition is reached in the experiments, but as a result of LV pressure-overloading. This assumption may not be valid when G&R is decompensatory; i.e., when hypertrophy is insufficient to mitigate the increase in pressure. Nevertheless, the general quantitative agreement between the data points and the prediction of the simplified model provides a certain level of confidence of the model hypothesis and its functional form.

5.1.2 Model Calibration and Validation—To calibrate the model parameter K (growth rate), longitudinal data of the LV geometry of more than 2 time points during G&R is required. In order to accommodate for interspecies differences in experiments, it may also be helpful to fit the G&R constitutive model in Eq. (1) using physiological time t_p rather than the chronological time t_c, based on the allometric scaling law $t_p = t_c\, W^{-1/4}$ with W denoting the body weight[79]. As an example, we fit the model to the experimental longitudinal data of neonatal rats acquired up to 150 days after birth. To do so, we assumed that the fetal pressure is 1/10 of that in the adult rat that has an LV pressure of 120 mm Hg ($\bar{P} = 9$)[80], and a thickness-to-radius ratio of $\bar{h} = 0.43$ (pre-growth wall LV thickness and internal radius of 0.65mm and 1.5mm, respectively). We find that a growth rate $K = 6 \times 10^{-4}$/ day is able to fit the experimental longitudinal data of neonatal rats relatively well[80]. As shown in Figure 4b, the parabolic growth curve predicted by the model is consistent with the trend found in the experimental data. In the final step to ascertain the predictive capability of the parameterized model, the calibrated growth rate of $K = 6 \times 10^{-4}$/ day needs to be validated against an independent set of measurements that are not used in the calibration process. Sampling techniques such as random subsampling, K-fold cross-validation and leave-one-out-cross-validation can be used to overcome the limitation of a small set of experimental data.[81,82]

Using a simplified model, we have demonstrated the two important aspects of G&R mathematical model development; i.e., model hypothesis testing and model validation/calibration. In the former, we seek to test whether the model hypothesis and formulation are consistent with existing experimental data, while in the latter, we seek to determine and test parameter values that best-fit the data. The illustrated example also demonstrates the potentiality of approaching the issue of model calibration and validation in a systematic way: (1) reducing the model to its simplest form suitable for validation and calibration, (2) calibrating the simplified model and (3) using the calibrated parameter values as initial guesses for the calibration of a more sophisticated model with realistic ventricular geometry. In this process, one may also find that the model may be inadequate to explain certain features of the experiments and if so, appropriate refinement or reformulation of the model then becomes necessary. For example, a hypothetical scenario where the model prediction of the change in thickness $\Delta\bar{h}$ for a given change in pressure $\bar{P}$ is substantially and consistently higher than those found in the experiment (i.e., when all the experimental data points lie below the curves in Figure 4a) would imply that a change in thickness during G&R is

insufficient to normalize the wall stress. In that case, the model would need to be reformulated (e.g., if G&R shows better correlation with another stimulant such as strain or strain energy) or refined (e.g., if experiments imply that there exists a threshold for cellular hypertrophy – See Figure 4c for a hypothetical example). In the latter case, new parameters (e.g., a threshold for hypertrophy) would need to be introduced into the model.

5.2 Model integrations across scales

As discussed, a clear distinction can be found in existing mathematical models of G&R that have focused on either the associated biochemical reactions or mechanics. There is still a disconnection between these two types of models, especially in terms of the spatial and temporal scales. Biochemical models of G&R were largely constructed based on experiments conducted using *in vitro* cell culture studies usually lasting a few days, whereas the mechanics models of G&R were largely constructed based on *in vivo* animal studies usually lasting for a few weeks.

These different mathematical models need to be integrated to achieve a system understanding of G&R under both physiological and pathological conditions. This is especially so because mechanics-based models can provide physiologically realistic input such as animal or patient-specific myocardial strain/stress to the biochemical models, whereas biochemical models can provide a more physical G&R signaling pathways for the mechanics-based models. The integration can be achieved via a simple relation between the parameters of the two different models (e.g., biochemical reaction rates -> growth rate) or a complete integration of the biochemical model to the mechanics-based model as illustrated in Figure 5.

5.3 A need for multiscale G&R modeling

It is clear that a multiscale G&R model can be a potentially useful research and clinical tool. Specifically, such a model can be useful in (1) developing a more in-depth understanding of the various G&R mechanisms, and in future, (2) a tool personalized treatment. The connection of G&R models of different timescale is essential in predicting how short term (acute) events can influence the long-term (chronic) course of a disease and/or treatment. On the other hand, connecting G&R models at different spatial scales will enable one to predict the large-scale effects arising from small-scale molecular events. A multiscale G&R model has the potential to unravel how minute changes at the small-scale level can lead to significant long-term large-scale changes, which is analogous to the so-called “butterfly effects”[b] in Chaos theory[83]. Such a model would be especially useful in understanding and predicting the progression of a number of heart diseases and potential treatments. We discuss two areas where such a multiscale G&R could potentially be useful.

Cardiac resynchronization therapy—Reverse remodeling in the form of a reduction in LV end-systolic volume (by ≥ 15%) is a clinically-relevant indicator of a positive response to cardiac resynchronization therapy (CRT)[84]. Approximately, 30% of patients, however, do

[b]The “butterfly effect” is a term coined by the mathematician Edward Lorenz in describing how a slight variation in the initial conditions of a complex nonlinear system can have a tremendous impact on the future outcomes. To describe this phenomenon, he gave an example of how the flapping of a butterfly’s wing in Brazil can set off a tornado in Texas.

not improve after therapy and the identification of potential responders to CRT remains a challenge. One of the hypothesis is that CRT can help to attenuate the early systolic stretch, a potential G&R stimulant, found in the late activated region as a result of left branch bundle block[85]. This effect can become confounded, however, by other factors such as a depressed contractility in ischemic patients. Computational modeling, with its inherent ability to integrate all the confounding factors, have already been used to understand the short-term effects of this treatment[86]. A multiscale G&R model could potentially be used to understand and predict the long-term effects of CRT.

Familial Hypertrophic Cardiomyopathy—Familial hypertrophic cardiomyopathy is a disease associated with the genetic mutation of sarcomeric proteins[87]. Some of the features associated with this disease include myocyte hypertrophy and disarray, fibrosis, diastolic dysfunction, and thickening of the ventricular wall. These genetic mutations can alter sarcomere function, which support some of the prevailing hypotheses that the resultant large-scale G&R features are compensatory responses to this alteration.[87] In this aspect, a multiscale G&R model that is able to connect small-scale molecular-level changes caused by mutation to large-scale ventricular G&R features could be extremely useful in testing these hypotheses. Given that pharmacological drugs operate at the molecular level, such a multiscale model could, in principle, be also used as an in silico clinical trial to test the long-term efficacy of new drugs.

6. Conclusion

Since the first observation by Sandler and Dodge[88], who speculated that the "*heart may hypertrophy as a result of increased tension to maintain wall stress within certain limits as yet undefined*", the past 50 years has seen significant advances in our knowledge about G&R in the myocardium. Indeed, it is becoming clearer that myocardial G&R is a very complex process – its mechanism is certainly not as simple as the one originally suggested by Sandler and Dodge[88]. There is little doubt that mathematical modeling can play an important role in our quest to elucidate the complex mechanisms of G&R. There are many challenges in improving the current state of mathematical cardiac G&R models and synergistically integrating them with experiments and clinical data. Overcoming these challenges will require significant effort. But with heart failure still affecting a large population, the benefits are likely to be enormous.

Acknowledgments

The authors thank Pamela Derish in the Department of Surgery, UCSF, for proofreading the manuscript. This work was supported by NIH Grants R01-HL-077921 (J.M. Guccione) and R01-HL-118627 and U01-HL-119578 (J.M. Guccione and G.S. Kassab).

Appendix

Derivation of simplified G&R constitutive model for pressure overload

The simplified constitutive law was derived from previous 3D constitutive models of stress-mediated G&R[53,73]. Those models were constructed based on the hypothesis that G&R

occurs for the purpose of restoring ventricular wall stress. A simplified version of these models can be written as follows:

$$\frac{\dot{\Delta h}}{r_i} = K(\sigma - \sigma^*) \quad \text{(A1)}$$

Here, $\Delta h/r_i$ is the change in thickness during G&R normalized with respect to the pre-growth LV inner radius. This quantity has the same physical meaning as the growth deformation gradient tensor in the volumetric G&R framework. In Equation (A1), K is the growth rate constant, σ is the wall stress as a result of a new pressure P_{new}, and σ* is the wall stress in the pre-growth configuration under the previous pressure P_{old}, which can be assumed to be a homeostatic set point. Using Laplace's law and assuming that (1) the LV can be described by an ellipsoid, (2) the cavity volume does not change (i.e., r_i is a constant) and (3) a thick ventricular wall with homogeneous stress distribution across the thickness, the pre- and post-growth meridional wall stresses can be approximated as[89,90]

$$\sigma^* = \frac{P_{\text{old}}}{2\frac{h}{r_i}(1+\frac{h}{2r_i})}; \quad \sigma^* = \frac{P_{\text{new}}}{2(\frac{h+\Delta h}{r_i})(1+\frac{h+\Delta h}{2r_i})}. \quad \text{(A2,3)}$$

Although one can also compute for the circumferential wall stress here, the calculation requires information about the LV major- and minor-axis dimensions. These information are not given in most of the experimental studies.

Letting $\bar{h} = h/r_i$, $\Delta\bar{h} = \Delta h/r_i$, $\bar{P} = (P_{\text{new}} - P_{\text{old}})/P_{\text{old}}$, and substituting (A2) and (A3) into (A1) yields

$$\dot{\Delta\bar{h}} = KP_o\left(\frac{1+\bar{P}}{(\bar{h}+\Delta\bar{h})(2+\bar{h}+\Delta\bar{h})} - \frac{1}{\bar{h}(2+\bar{h})}\right). \quad \text{(A4)}$$

Equation (A4) can be solved with an initial condition of $\Delta\bar{h} = 0$ to obtain a time-evolution of the wall thickness. At steady state, $\dot{\Delta\bar{h}} = 0$ and the change in wall thickness $\Delta\bar{h}$ can be computed from Equation (A4) as a function of $\bar{P}$ and $\bar{h}$ by:

$$\Delta\bar{h} = -1 - \bar{h} + \sqrt{1+2\bar{h}+2\bar{P}\bar{h}+\bar{h}^2+\bar{P}\bar{h}^2} \quad \text{(A5)}$$

We note that two solutions exist for $\Delta\bar{h}$ in Eq. (A4) under a steady state condition. However, only one solution yields a physically meaningful ($\Delta\bar{h} > 0$) solution.

Table A1

Experimental measurements of the long-term LV geometrical changes due to pressure overload of various species from the literature.

Species	P_{old} (mmHg)	P_{new} (mmHg)	$\bar{P}$	r_i (mm)	h (mm)	Δh (mm)	$\bar{h}$	$\Delta\bar{h}$
Rats	115	197	0.71	2.45	2.8	0.8	1.14	0.33
Humans	117	220	0.88	24.00	9.0	8.0	0.38	0.33

Species	P_{old} (mmHg)	P_{new} (mmHg)	$\bar{P}$	r_i (mm)	h (mm)	Δh (mm)	$\bar{h}$	$\bar{\Delta h}$
Swine	134	179	0.34	12.50	8.9	1.1	0.71	0.09
Lamb	95	145	0.53	12.00	10.0	4.0	0.83	0.33
Sheep	110	142	0.29	17.00	14.0	3.0	0.82	0.18
Guinea pigs	71	88	0.24	2.26	2.6	0.2	1.15	0.09
Guinea pigs	62	115	0.85	2.33	2.6	0.2	1.12	0.09

Note: r_i in the results from the guinea pigs are calculated from LV cavity area measurements.

References

1. Weber KT, Brilla CG. Pathological hypertrophy and cardiac interstitium. Fibrosis and renin-angiotensin-aldosterone system. Circulation. 1991; 83(6):1849–1865. [PubMed: 1828192]
2. Cohn JN, Ferrari R, Sharpe N. Cardiac remodeling—concepts and clinical implications: a consensus paper from an international forum on cardiac remodeling. J. Am. Coll. Cardiol. 2000; 35(3):569–582. [PubMed: 10716457]
3. White HD, Norris RM, Brown MA, Brandt PW, Whitlock RM, Wild CJ. Left ventricular end-systolic volume as the major determinant of survival after recovery from myocardial infarction. Circulation. 1987; 76(1):44–51. [PubMed: 3594774]
4. Hamer AW, Takayama M, Abraham KA, Roche AH, Kerr AR, Williams BF, Ramage MC, White HD. End-systolic volume and long-term survival after coronary artery bypass graft surgery in patients with impaired left ventricular function. Circulation. 1994; 90(6):2899–2904. [PubMed: 7994836]
5. Levin H, Oz M, Chen J, Packer M, Rose E, Burkhoff D. Reversal of chronic ventricular dilation in patients with end-stage cardiomyopathy by prolonged mechanical unloading. Circulation. 1995; 91(11):2717–2720. [PubMed: 7758175]
6. Burkhoff D, Klotz S, Mancini DM. LVAD-induced reverse remodeling: basic and clinical implications for myocardial recovery. J. Card. Fail. 2006; 12(3):227–239. [PubMed: 16624689]
7. Williams AR, Trachtenberg B, Velazquez DL, McNiece I, Altman P, Rouy D, Mendizabal AM, Pattany PM, Lopera GA, Fishman J, Zambrano JP, Heldman AW, Hare JM. Intramyocardial stem cell injection in patients with ischemic cardiomyopathy: Functional recovery and reverse remodeling. Circ. Res. 2011; 108:792–796. [PubMed: 21415390]
8. Lee LC, Wall ST, Klepach D, Ge L, Zhang Z, Lee RJ, Hinson A, Gorman JH, Gorman RC, Guccione JM. Algisyl-LVR™ with coronary artery bypass grafting reduces left ventricular wall stress and improves function in the failing human heart. Int. J. Cardiol. 2013; 168:2022–2028. [PubMed: 23394895]
9. Yu CM, Bleeker GB, Fung JWH, Schalij MJ, Zhang Q, van der Wall EE, Chan YS, Kong SL, Bax JJ. Left ventricular reverse remodeling but not clinical improvement predicts long-term survival after cardiac resynchronization therapy. Circulation. 2005; 112:1580–1586. [PubMed: 16144994]
10. Yu CM, Fung W-H, Lin H, Zhang Q, Sanderson JE, Lau CP. Predictors of left ventricular reverse remodeling after cardiac resynchronization therapy for heart failure secondary to idiopathic dilated or ischemic cardiomyopathy. Am J Cardiol. 2003; 91:684–688. [PubMed: 12633798]
11. Omens JH. Stress and strain as regulators of myocardial growth. Prog. Biophys. Mol. Biol. 1998; 69(2–3):559–572. [PubMed: 9785956]
12. Omens JH, McCulloch AD, Lorenzen-schmidt I. Mechanotransduction in Cardiac Remodeling and Heart Failure. 2007
13. Sheehy SP, Grosberg A, Parker KK. The contribution of cellular mechanotransduction to cardiomyocyte form and function. Biomech. Model. Mechanobiol. 2012; 11(8):1227–1239. [PubMed: 22772714]
14. Holmes JW. Candidate mechanical stimuli for hypertrophy during volume overload. J. Appl. Physiol. 2004 May.97:1453–1460. 2004. [PubMed: 15169750]

15. Grossman W. Cardiac Hypertrophy : Pathologic Process? Useful Adaptation or. Am. J. Med. 1980 Oct.69:576–584. [PubMed: 6448546]
16. Kehat I, Molkentin JD. Molecular pathways underlying cardiac remodeling during pathophysiological stimulation. Circulation. 2010; 122(25):2727–2735. [PubMed: 21173361]
17. Pfeffer MA, Braunwald E. Ventricular remodeling after myocardial infarction. Experimental observations and clinical implications. Circulation. 1990; 81:1161–1172. [PubMed: 2138525]
18. Vliegen HW, van der Laarse A, Cornelisse CJ, Eulderink F. Myocardial changes in pressure overload-induced left ventricular hypertrophy. A study on tissue composition, polyploidization and multinucleation. Eur. Heart J. 1991; 12(4):488–494. [PubMed: 1829680]
19. Bergmann O, Bhardwaj RD, Bernard S, Zdunek S, Barnabé-Heider F, Walsh S, Zupicich J, Alkass K, Buchholz BA, Druid H, Jovinge S, Frisén J. Evidence for cardiomyocyte renewal in humans. Science. 2009; 324:98–102. [PubMed: 19342590]
20. Schaub MC, Hefti MA, Zuellig RA, Morano I. Modulation of contractility in human cardiac hypertrophy by myosin essential light chain isoforms. Cardiovasc. Res. 1998; 37(2):381–404. doi:S0008-6363(97)00258-7 [pii]. [PubMed: 9614495]
21. Kass DA, Bronzwaer JGF, Paulus WJ. What mechanisms underlie diastolic dysfunction in heart failure? Circ. Res. 2004; 94(12):1533–1542. [PubMed: 15217918]
22. Spinale FG. Myocardial matrix remodeling and the matrix metalloproteinases: influence on cardiac form and function. Physiol. Rev. 2007; 87(4):1285–12342. [PubMed: 17928585]
23. Weber KT. Cardiac Interstitium in Health and Disease : The Fibrillar Collagen Network. J. Am. Coll. Cardiol. 1989; 13(7):1637–1652. [PubMed: 2656824]
24. Robinson TF, Cohen-Gould L, Factor SM, Eghbali M, Blumenfeld OO. Structure and function of connective tissue in cardiac muscle: collagen types I and III in endomysial struts and pericellular fibers. Scanning Microsc. 1988; 2:1005–1015. [PubMed: 3399840]
25. King JH, Huang CLH, Fraser JA. Determinants of myocardial conduction velocity: Implications for arrhythmogenesis. Front. Physiol. 2013 Jun 4.:1–14. June. [PubMed: 23372552]
26. Nguyen TP, Qu Z, Weiss JN. Cardiac fibrosis and arrhythmogenesis: The road to repair is paved with perils. J. Mol. Cell. Cardiol. 2014; 70:83–91. [PubMed: 24184999]
27. Hefti MA, Harder BA, Eppenberger HM, Schaub MC. Signaling pathways in cardiac myocyte hypertrophy. J. Mol. Cell. Cardiol. 1997; 29(11):2873–2892. [PubMed: 9405163]
28. Cooling M, Hunter P, Crampin EJ. Modeling hypertrophic IP3 transients in the cardiac myocyte. Biophys. J. 2007; 93(10):3421–3433. [PubMed: 17693463]
29. Shin SY, Choo SM, Kim D, Baek SJ, Wolkenhauer O, Cho KH. Switching feedback mechanisms realize the dual role of MCIP in the regulation of calcineurin activity. FEBS Lett. 2006; 580(25): 5965–5973. [PubMed: 17046757]
30. Novak IL, Slepchenko BM, Mogilner A, Loew LM. Cooperativity between cell contractility and adhesion. Phys. Rev. Lett. 2004; 93(26 I):2–5.
31. Grosberg A, Kuo P-L, Guo C-L, Geisse Na, Bray M-A, Adams WJ, Sheehy SP, Parker KK. Self-organization of muscle cell structure and function. PLoS Comput. Biol. 2011; 7(2):e1001088. [PubMed: 21390276]
32. Deshpande VS, Mrksich M, McMeeking RM, Evans AG. A bio-mechanical model for coupling cell contractility with focal adhesion formation. J. Mech. Phys. Solids. 2008; 56(4):1484–1510.
33. Ryall KA, Holland DO, Delaney Ka, Kraeutler MJ, Parker AJ, Saucerman JJ. Network reconstruction and systems analysis of cardiac myocyte hypertrophy signaling. J. Biol. Chem. 2012; 287(50):42259–42268. [PubMed: 23091058]
34. Bueno OF, De Windt LJ, Tymitz KM, Witt SA, Kimball TR, Klevitsky R, Hewett TE, Jones SP, Lefer DJ, Peng CF, Kitsis RN, Molkentin JD. The MEK1-ERK1/2 signaling pathway promotes compensated cardiac hypertrophy in transgenic mice. EMBO J. 2000; 19(23):6341–6350. [PubMed: 11101507]
35. Molkentin JD, Dorn GW. Cytoplasmic signaling pathways that regulate cardiac hypertrophy. Annu. Rev. Physiol. 2001; 63:391–426. [PubMed: 11181961]
36. Majkut S, Dingal PCDP, Discher DE. Stress sensitivity and mechanotransduction during heart development. Curr. Biol. 2014; 24(10):R495–R501. [PubMed: 24845682]

37. Karagiannis ED, Popel AS. A theoretical model of type I collagen proteolysis by matrix metalloproteinase (MMP) 2 and membrane type 1 MMP in the presence of tissue inhibitor of metalloproteinase 2. J. Biol. Chem. 2004; 279(37):39105–39114. [PubMed: 15252025]
38. Vempati P, Karagiannis ED, Popel AS. A biochemical model of matrix metalloproteinase 9 activation and inhibition. J. Biol. Chem. 2007; 282(52):37585–37596. [PubMed: 17848556]
39. Jin YF, Han HC, Berger J, Dai Q, Lindsey ML. Combining experimental and mathematical modeling to reveal mechanisms of macrophage-dependent left ventricular remodeling. BMC Syst. Biol. 2011; 5(1):60. [PubMed: 21545710]
40. Lindsey ML, Escobar GP, Dobrucki LW, Goshorn DK, Bouges S, Mingoia JT, McClister DM, Su H, Gannon J, MacGillivray C, Lee RT, Sinusas AJ, Spinale FG. Matrix metalloproteinase-9 gene deletion facilitates angiogenesis after myocardial infarction. Am. J. Physiol. Heart Circ. Physiol. 2006; 290(1):H232–H239. [PubMed: 16126817]
41. Yang F, Liu Y, Yang X, Xu J, Kapke A, Carretero OA. Myocardial infarction and cardiac remodelling in mice. Exp. Physiol. Transl. Integr. 2002; 87(5):547–555.
42. Fang L, Gao XM, Moore XL, Kiriazis H, Su Y, Ming Z, Lim YL, Dart AM, Du XJ. Differences in inflammation, MMP activation and collagen damage account for gender difference in murine cardiac rupture following myocardial infarction. J. Mol. Cell. Cardiol. 2007; 43(5):535–544. [PubMed: 17689559]
43. Gajarsa JJ, Kloner RA. Left ventricular remodeling in the post-infarction heart: a review of cellular, molecular mechanisms, and therapeutic modalities. Heart Fail. Rev. 2011; 16(1):13–21. [PubMed: 20623185]
44. Arts T, Prinzen FW, Snoeckx LHEH, Rijcken JM, Reneman RS. Adaption of cardiac structure by mechanical feedback in the environment of the cell: A model study. Biophys. J. 1994; 66(4):953–961. [PubMed: 8038399]
45. Kroon W, Delhaas T, Bovendeerd PHM, Arts T. Computational analysis of the myocardial structure: Adaptation of cardiac myofiber orientations through deformation. Med. Image Anal. 2009; 13(2):346–353. [PubMed: 18701341]
46. Bovendeerd PHM. Modeling of cardiac growth and remodeling of myofiber orientation. J. Biomech. 2012; 45(5):872–881. [PubMed: 22169149]
47. Rodriguez E, Hoger A, Mcculloch AD. Stress-dependent finite growth in soft elastic tissues. J. Biomech. 1994; 27(4):455–467. [PubMed: 8188726]
48. Lee EH. Elastic-Plastic Deformation at Finite Strains. J. Appl. Mech. 1969; 36(1):1–6.
49. Genet M, Rausch MK, Lee LC, Choy JS, Zhao X, Kassab GS, Kozerke S, Guccione JM, Kuhl E. Heterogeneous growth-induced prestrain in the heart. J. Biomech. 2015 (In press).
50. Omens JH, Fung YC. Residual strain in rat left ventricle. Circ. Res. 1990; 66:37–45. [PubMed: 2295143]
51. Lanir Y. Mechanisms of residual stress in soft tissues. J. Biomech. Eng. 2009; 131(4):044506. [PubMed: 19275448]
52. Lanir Y, Hayam G, Abovsky M, Zlotnick AY, Uretzky G, Nevo E, Ben-Haim SA. Effect of myocardial swelling on residual strain in the left ventricle of the rat. Am. J. Physiol. 1996; 270(5 Pt 2):H1736–H1743. [PubMed: 8928881]
53. Lin IE, Taber LA. A model for stress-induced growth in the developing heart. J. Biomech. Eng. 1995; 117(3):343–349. [PubMed: 8618388]
54. Taber LA, Chabert S. Theoretical and experimental study of growth and remodeling in the developing heart. Biomech. Model. Mechanobiol. 2002; 1(1):29–43. [PubMed: 14586705]
55. Taber LA. Towards a unified theory for morphomechanics. Philos. Trans. A. Math. Phys. Eng. Sci. 2009; 367(1902):3555–3583. [PubMed: 19657011]
56. Kerckhoffs RCP. Computational modeling of cardiac growth in the post-natal rat with a strain-based growth law. J. Biomech. 2012; 45(5):865–871. [PubMed: 22169150]
57. Kroon W, Delhaas T, Arts T, Bovendeerd P. Computational modeling of volumetric soft tissue growth: application to the cardiac left ventricle. Biomech. Model. Mechanobiol. 2009; 8(4):301–309. [PubMed: 18758835]
58. Taber LA. Biomechanics of Growth, Remodeling, and Morphogenesis. Appl. Mech. Rev. 1995; 48(8):487–545.

59. Göktepe S, Abilez OJ, Parker KK, Kuhl E. A multiscale model for eccentric and concentric cardiac growth through sarcomerogenesis. J. Theor. Biol. 2010; 265(3):433–442. [PubMed: 20447409]
60. Lee LC, Genet M, Acevedo-Bolton G, Ordovas K, Guccione JM, Kuhl E. A computational model that predicts reverse growth in response to mechanical unloading. Biomech. Model. Mechanobiol. 2015; 14:217–229. [PubMed: 24888270]
61. Lee LC, Sundnes J, Genet M, Wenk JF, ST W. An Integrated Electromechanical-Reversible Growth Heart Model for Simulating Cardiac Therapies. Biomech. Model. Mechanobiol. 2015 (In press).
62. Kerckhoffs RCP, Omens J, McCulloch AD. A single strain-based growth law predicts concentric and eccentric cardiac growth during pressure and volume overload. Mech. Res. Commun. 2012; 42:40–50. [PubMed: 22639476]
63. Emery JL, Omens JH. Mechanical regulation of myocardial growth during volume-overload hypertrophy in the rat. Am. J. Physiol. 1997; 273(3 Pt 2):H1198–H1204. [PubMed: 9321807]
64. Guterl KA, Haggart CR, Janssen PM, Holmes JW. Isometric contraction induces rapid myocyte remodeling in cultured rat right ventricular papillary muscles. Am. J. Physiol. Heart Circ. Physiol. 2007; 293(6):H3707–H3712. [PubMed: 17921334]
65. Weber KT, Anversa P, Armstrong PW, Brilla CG, Burnett JC, Cruickshank JM, Devereux RB, Giles TD, Korsgaard N, Leier CV, Mendelsohn FAO, Motz WH, Mulvany MJ, Strauer BE. Remodeling and Raparation of the Cardiovascular System. J. Am. Coll. Cardiol. 1992; 20(1):3–16. [PubMed: 1318886]
66. Rain S, Handoko L, Trip P, Gan T-J, Westerhof N, Stienen G, Paulus W, Ottenheijm C, Marcus T, Dorfmüller P, Guignabert C, Humbert M, MacDonald P, dos Remedios C, Postmus P, Saripalli C, Hidalgo C, Granzier H, Vonk-Noordegraaf A, van der Velden J, de Man F. Right Ventricular Diastolic Impairment in Patients With Pulmonary Arterial Hypertension. Circulation. 2013; 128:2016–2025. doi: [PubMed: 24056688]
67. Shimkunas R, Makwana O, Spaulding K, Bazargan M, Khazalpour M, Takaba K, Soleimani M, Myagmar B-E, Lovett DH, Simpson PC, Ratcliffe MB, Baker AJ. Myofilament dysfunction contributes to impaired myocardial contraction in the infarct border zone. AJP Hear. Circ. Physiol. 2014; 307:H1150–H1158.
68. Humphrey JD, Rajagopal KR. A Constrained Mixture Model for Growth and Remodeling of Soft Tissues. Math. Model. Methods Appl. Sci. 2002; 12:407–430.
69. Baek S, Rajagopal KR, Humphrey JD. A Theoretical Model of Enlarging Intracranial Fusiform Aneurysms. J. Biomech. Eng. 2006; 128(1):142. [PubMed: 16532628]
70. Valentín A, Holzapfel GA. Constrained mixture models as tools for testing competing hypotheses in arterial biomechanics: A brief survey. Mech. Res. Commun. 2012; 42:126–133. [PubMed: 22711947]
71. Gleason RL, Humphrey JD. Effects of a sustained extension on arterial growth and remodeling: A theoretical study. J. Biomech. 2005; 38:1255–1261. [PubMed: 15863110]
72. Ateshian GA, Humphrey JD. Continuum mixture models of biological growth and remodeling: past successes and future opportunities. Annu. Rev. Biomed. Eng. 2012; 14:97–111. [PubMed: 22809138]
73. Göktepe S, Abilez OJ, Parker KK, Kuhl E. A multiscale model for eccentric and concentric cardiac growth through sarcomerogenesis. J. Theor. Biol. 2010; 265(3):433–442. [PubMed: 20447409]
74. Litwin SE, Katz SE, Weinberg EO, Lorell BH, Aurigemma GP, Douglas PS. Serial echocardiographic-Doppler assessment of left ventricular geometry and function in rats with pressure-overload hypertrophy. Chronic angiotensin-converting enzyme inhibition attenuates the transition to heart failure. Circulation. 1995; 91(10):2642–2654. [PubMed: 7743628]
75. Grossman W, Jones D, McLaurin LP. Wall stress and patterns of hypertrophy in the human left ventricle. J. Clin. Invest. 1975; 56(1):56–64. [PubMed: 124746]
76. Nediani C, Formigli L, Perna AM, Ibba-Manneschi L, Zecchi-Orlandini S, Fiorillo C, Ponziani V, Cecchi C, Liguori P, Fratini G, Nassi P. Early changes induced in the left ventricle by pressure overload. An experimental study on swine heart. J. Mol. Cell. Cardiol. 2000; 32(1):131–142. [PubMed: 10652197]

77. Aoyagi T, Mirsky I, Flanagan MF, Currier JJ, Colan SD, Fujii AM. Myocardial function in immature and mature sheep with pressure-overload hypertrophy. Am. J. Physiol. 1992; 262(4 Pt 2):H1036–H1048. [PubMed: 1348910]

78. Laviolle B, Pape D, Verdier M-C, Lavenu A, Bellissant E. Hemodynamic and histomorphometric characteristics of heart failure induced by aortic stenosis in the guinea pig: comparison of two constriction sizes. Can. J. Physiol. Pharmacol. 2009; 87(11):908–914. [PubMed: 19935898]

79. Schmid-Nielson, K. Scaling: Why Is Animal Size so Important?. 1st. Cambridge University Press; 1984.

80. Anversa P, Olivetti G. Cellular basis of physiological and pathological myocardial growth. Compr. Physiol. 2011:75–144.

81. Stone M. Cross-Validatory Choice and Assessment of Statistical Predictions. J. R. Stat. Soc. Ser. B. 1974; 36:111–147.

82. Klipp E, Herwig R, Kowald A, Wierling C, Lehrach H. Systems Biology in Practice: Concepts, Implementation and Application. 2005

83. Lorenz EN. The Essence of Chaos. Am. J. Phys. 1995; 63(9):862.

84. Chung ES, Leon AR, Tavazzi L, Sun JP, Nihoyannopoulos P, Merlino J, Abraham WT, Ghio S, Leclercq C, Bax JJ, Yu CM, Gorcsan J, St John Sutton M, De Sutter J, Murillo J. Results of the Predictors of Response to CRT (PROSPECT) trial. Circulation. 2008; 117(20):2608–2616. [PubMed: 18458170]

85. Prinzen FW, Cheriex EC, Delhaas T, Van Oosterhout MFM, Arts T, Wellens HJJ, Reneman RS. Asymmetric thickness of the left ventricular wall resulting from asynchronous electric activation: A study in dogs with ventricular pacing and in patients with left bundle branch block. Am. Heart J. 1995; 130:1045–1053. [PubMed: 7484735]

86. Kerckhoffs RCP, Lumens J, Vernooy K, Omens JH, Mulligan LJ, Delhaas T, Arts T, McCulloch AD, Prinzen FW. Cardiac resynchronization: Insight from experimental and computational models. Prog. Biophys. Mol. Biol. 2008; 97:543–561. [PubMed: 18417196]

87. Cirino AL. Familial Hypertrophic Cardiomyopathy Overview. GeneReviews. 2008

88. Sandler H, Dodge HT. Left Ventricular Tension and Stress in Man. Circ. Res. 1971; XIII(2):437–445.

89. Falsetti HL, Mates RE, Grant C, Greene DG, Bunnell IL. Left Ventricular Wall Stress Calculated from One-Plane Cineangiography: an approach to force-velocity in man. Circ. Res. 1970; 26(1): 71–83. [PubMed: 5410094]

90. Yin FC. Ventricular wall stress. Circ. Res. 1981; 49(4):829–842. [PubMed: 7023741]

91. Wilson JS, Baek S, Humphrey JD. Parametric study of effects of collagen turnover on the natural history of abdominal aortic aneurysms. Proc. Math. Phys. Eng. Sci. 2013; 469:20120556. [PubMed: 23633905]

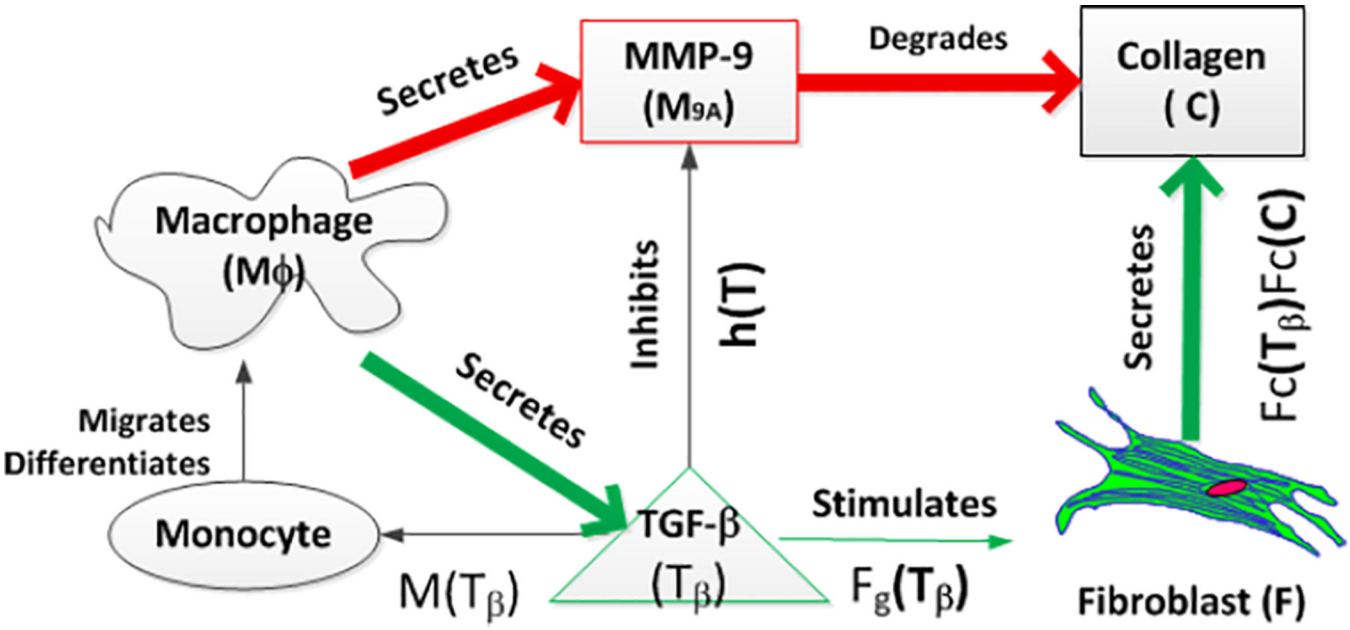

Figure 1.
Schematic of the biochemical pathways during scar formation as described by the mathematical model of Jin et al.[39]

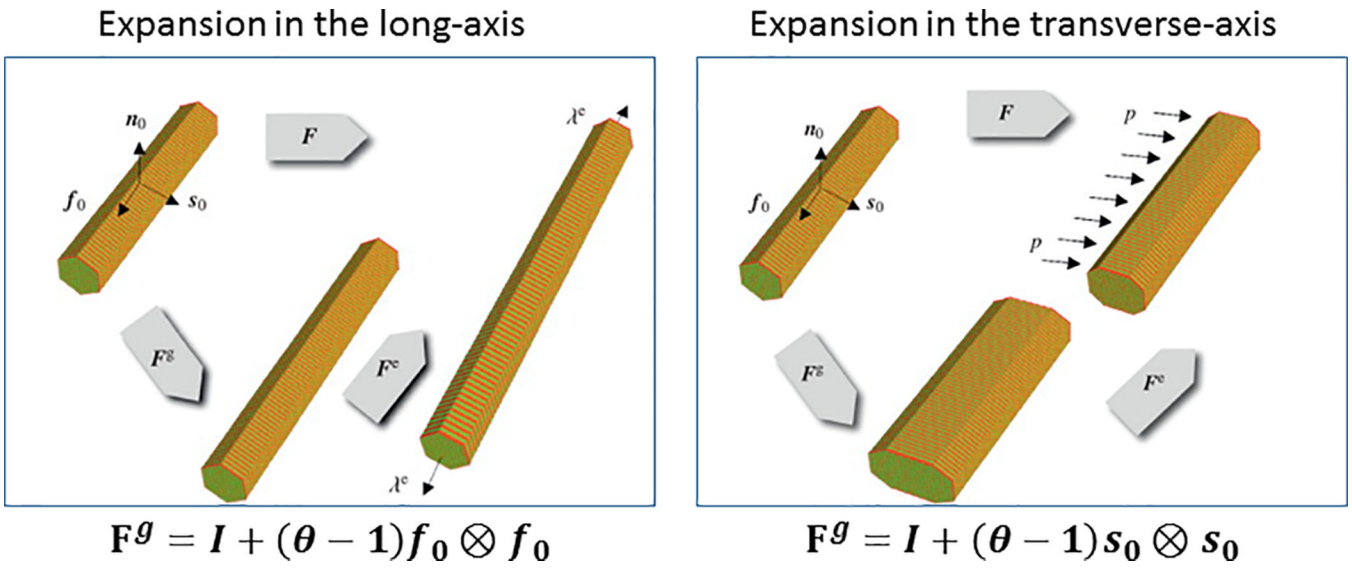

Figure 2.

Tensorial form of the growth deformation tensor $\mathbf{F}^g$ reflecting cellular shape changes. Adapted from Goktepe et al.[59]

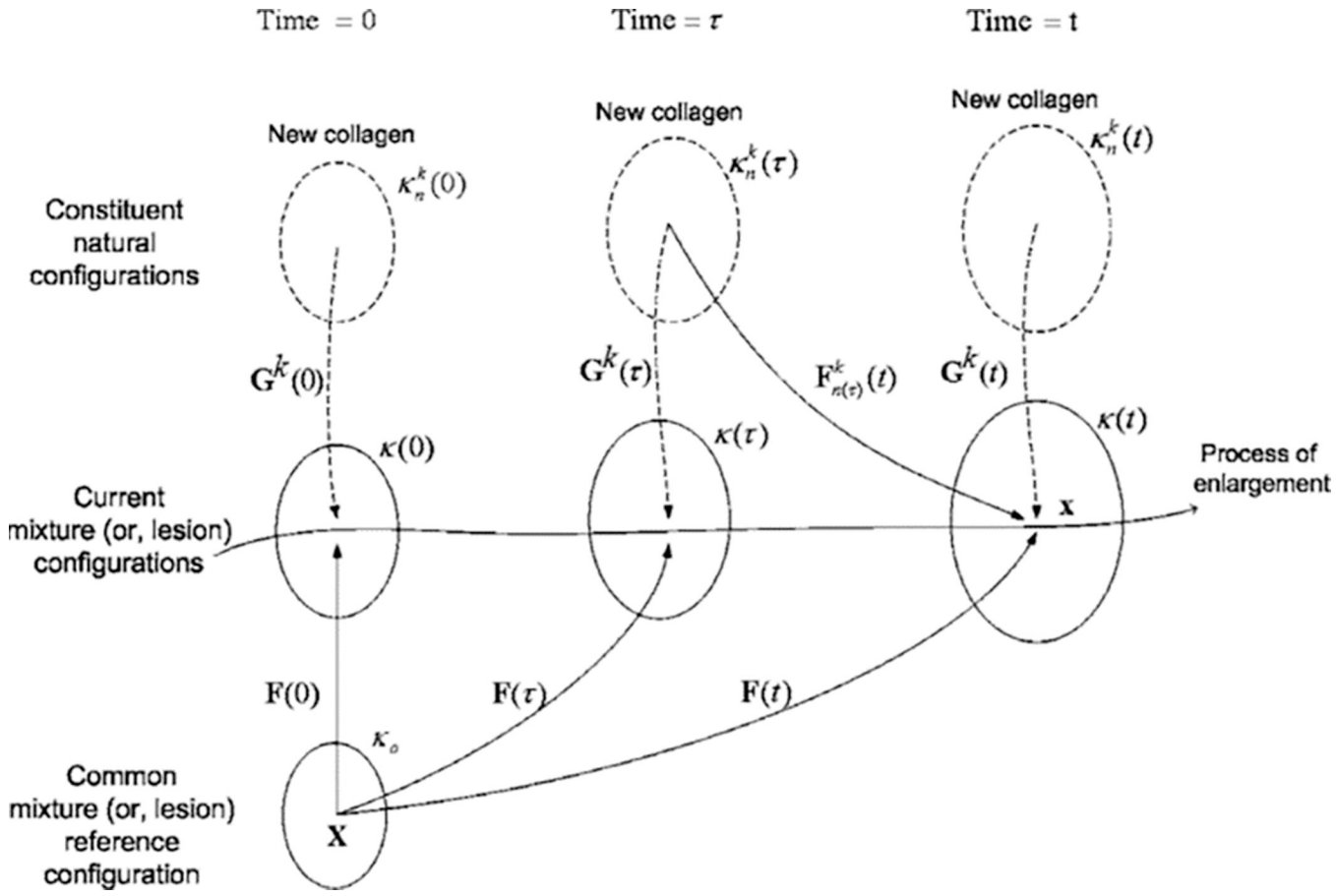

Figure 3.
Schematic of the constrained mixture-based G&R theory. Adapted from Baek et al.[69]

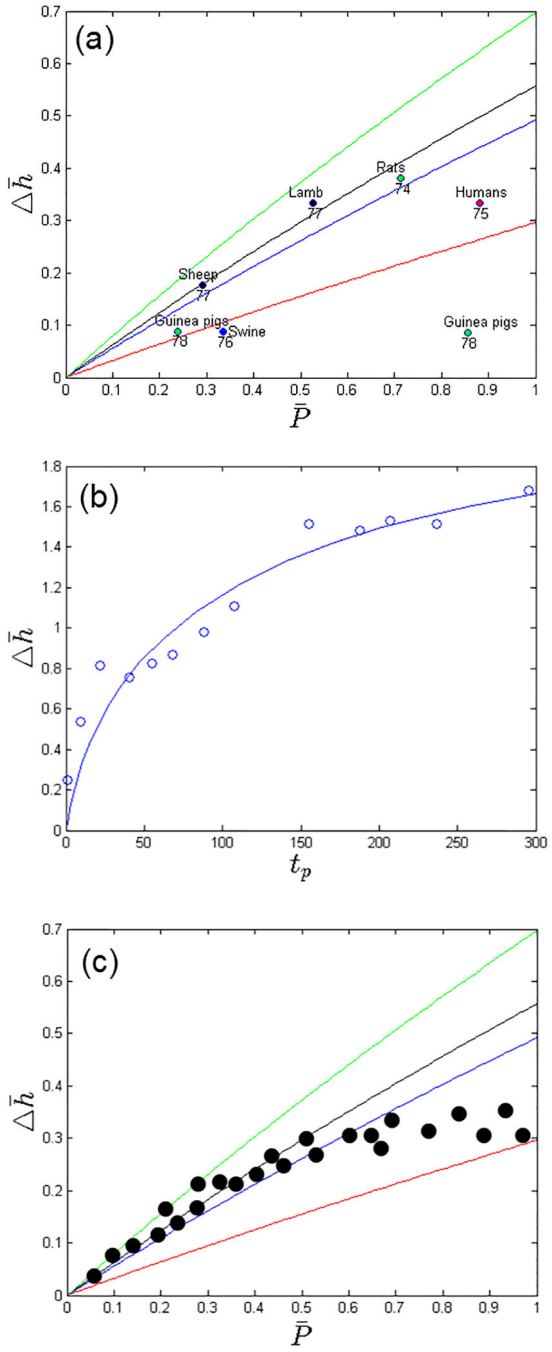

Figure 4.

(a): Normalized pressure change vs. thickness change as predicted by a simplified version of the G&R constitutive model at steady state (lines) and obtained from different experiments (dots). Reference numbers and species are given on the bottom and top of each experimental data point, respectively. **(b):** Wall thickness change vs. physiological time t_p in the fitted model (line) with experimental measurements in the neonatal rat heart (dots). Note: time-variable and wall thickness in the experimental data has been scaled to a physiological time t_p based on the body weight of 0.065kg and the internal LV radius of 1.5mm, respectively.

(c): Hypothetical example of experimental data (dots) showing the existence of a threshold for hypertrophy.

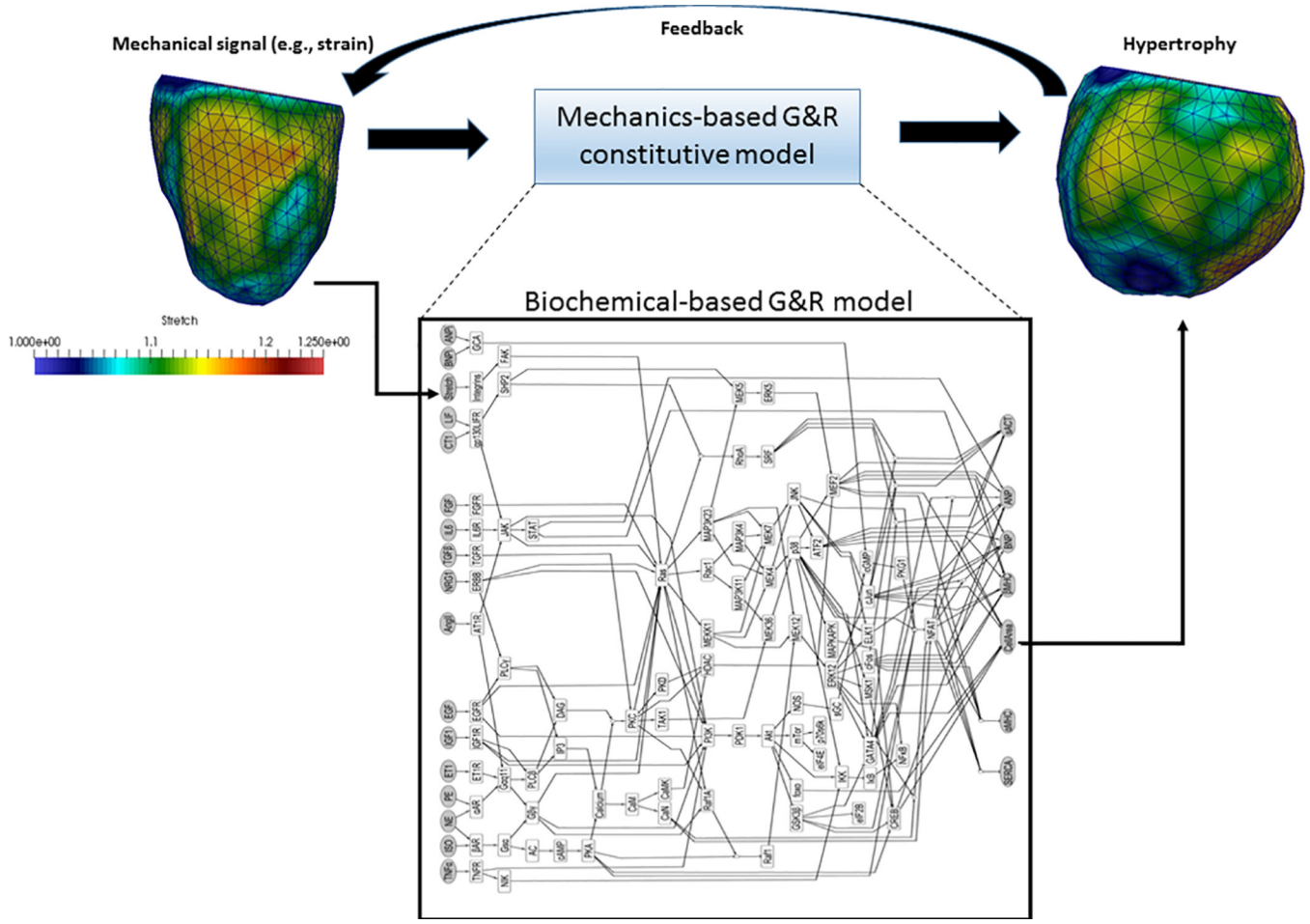

Figure 5.

An example of integrating a biochemical-based G&R model to a mechanics-based G&R model. In the example, the biochemical hypertrophic signaling network model is taken from Ryall et al.[33], with mechanical stretch as one of the inputs and the cell area as one of the outputs. These quantities can be associated with those from existing mechanics-based strain-mediated G&R constitutive models[60,62,73] in which mechanical strain and the growth deformation gradient tensor are the input and output, respectively. As such, the biochemical-based model can be integrated easily into mechanics-based G&R models.

Table 1

Parameters in the discussed myocardial G&R models

		Models	No. of parameters	BR	GM	LM	Remarks
Cellular-based	Hypertrophy	Rydall et al.[33]	>= 100	All	X	X	Note: Although all parameters listed here are biochemical reaction rates, it is unclear as to where the transition from biochemical to growth rates are in the model.
	ECM remodeling	Jin et al.[39]	15	3	9	3	
Continuum-based	Hypertrophy	Lin and Taber[53]	9	X	9	X	Focused on developmental G&R
		Goktepe et al.[73]	8	X	2	6	Assumed a different set of parameters for stress and strain-mediated G&R constitutive laws
		Lee et al.[60]	8	X	2	6	Assumed a different set of parameters for atrophy and hypertrophy
		Kerckhoff et al.[62]	15	X	6	4	
	ECM remodeling	Wilson et al.[91]	11	X	2	9	Parameters are associated with constituents in the arteries (collagen, elastin and smooth muscle). Only parameters associated with G&R are considered –parameters associated with the mechanical properties are listed here.

Abbreviations: BR, biochemical reaction rates; GM, growth/mass production rates; LM, limits/threshold/homeostatic states associated with G&R: ECM, extracellular matrix.